

DO-TH 96/08
May 1996

Probing the Parton Densities of Virtual Photons at ep Colliders

M. Glück, E. Reya and M. Stratmann

Institut für Physik, Universität Dortmund
D-44221 Dortmund, Germany

Abstract

The feasibility of an experimental determination of the parton distributions of virtual photons at high energy ep colliders is studied in the context of the DESY-HERA collider. Recently proposed parton densities of virtual photons are utilized to evaluate the appropriate production processes and their relevant kinematical regions. It is demonstrated that high E_T jet production with $E_T \simeq 5 - 7 \text{ GeV}$ and $b\bar{b}$ production can probe the parton distributions of virtual photons up to virtualities of a few GeV^2 . A useful leading order parametrization of our proposed photonic parton densities, suitable for further studies of these issues, is presented.

1 Introduction

The parton distributions of photons provide us with a unique opportunity to study the underlying mechanisms responsible for the specific shapes of hadronic parton distributions. This is due to the fact that in contrast to the situation with nucleons or pions the photon provides us with the possibility of investigating its parton distributions in a continuous range of masses (virtualities) $P^2 = -p_\gamma^2$ with p_γ denoting the four momentum of the photon emitted from, say, an electron in an e^+e^- or ep collider. (In the latter case it is common to use $Q^2 = -q^2$ instead of P^2 for denoting the photon's virtuality, but we prefer P^2 according to the original notation used in e^+e^- annihilations where it refers to the virtuality of the probed virtual target photon [1].) This is particularly interesting for models based on some specific notion concerning the nonperturbative origin of the hadronic parton distributions which quite naturally lead to rather unique expectations [1] concerning the P^2 dependence of the photonic parton distributions. Similar approaches have been presented recently [2, 3]. Studies of parton distributions of virtual ($P^2 \neq 0$) photons, $f^{\gamma(P^2)}(x, \mu_F^2)$ with some properly chosen factorization scale μ_F , may thus provide an important test of the underlying ideas. In the present paper we present predictions for production processes at the DESY-HERA ep collider which are highly sensitive to the 'resolved' components $f^{\gamma(P^2)}$. In particular the predicted rates for the 'resolved' production rates in these processes are presented in appropriate kinematical ranges suitable for testing the recently proposed [1-3] $f^{\gamma(P^2)}$. Detailed experimental tests of such predictions will obviously elucidate the so far unanswered question as to when a deep inelastic ep process is dominated by the usual 'direct' $\gamma^* \equiv \gamma(P^2)$ induced cross sections, not contaminated by the so far poorly known 'resolved' $f^{\gamma(P^2)}(x, \mu_F^2)$ contributions.

To introduce our notations and conventions we begin in Sec. 2 with a short presentation of the proposed model [1]. In Sec. 3 and 4 we present quantitative results for the electroproduction of heavy quarks and (single inclusive) jets, respectively, with detailed comparisons of the individual direct and resolved contributions of virtual photons. Our conclusions are drawn in Sec. 5. In the Appendix we present a LO-QCD parametrization

of our predicted distributions [1] which should be sufficient and useful for any forthcoming experimental or theoretical investigation as well as for eventual Monte Carlo analyses.

2 The Model

The basic ingredient of our model for the parton content of virtual transverse photons $\gamma(P^2)$ is that it should be smooth in P^2 at $P^2 = 0$ where previous results [4] for the real photon should hold, which are given at the low (dynamical) input scale $Q^2 = \mu^2$ by

$$f^\gamma(x, \mu^2) = \kappa (4\pi\alpha/f_\rho^2) f^\pi(x, \mu^2) \quad (2.1)$$

where $f = q, \bar{q}, g$ and with κ, f_ρ^2, μ^2 and $f^\pi(x, \mu^2)$ specified in [4] and [5], respectively. This is expected to hold for the leading order (LO) distributions as well as for the next-to-leading order (NLO) real photon $[\gamma \equiv \gamma(P^2 = 0)]$ distributions in the DIS_γ factorization scheme [6] which are related to the $\overline{\text{MS}}$ factorization scheme distributions via [4, 6]

$$f_{\text{DIS}_\gamma}^\gamma(x, Q^2) = f_{\overline{\text{MS}}}^\gamma(x, Q^2) + \delta f^\gamma(x) \quad (2.2)$$

with

$$\begin{aligned} \delta q^\gamma(x) = \delta \bar{q}^\gamma(x) &= 3e_q^2 \frac{\alpha}{2\pi} \left\{ [x^2 + (1-x)^2] \ln \frac{1-x}{x} - 1 + 8x - 8x^2 \right\} \\ \delta g^\gamma(x) &= 0 \quad . \end{aligned} \quad (2.3)$$

This, together with a VMD inspired P^2 dependence factor yields the following boundary conditions for $f^{\gamma(P^2)}(x, Q^2)$ at $Q^2 = \tilde{P}^2$:

$$f^{\gamma(P^2)}(x, \tilde{P}^2) = \eta(P^2) f_{\text{non-pert}}^{\gamma(P^2)}(x, \tilde{P}^2) + [1 - \eta(P^2)] f_{\text{pert}}^{\gamma(P^2)}(x, \tilde{P}^2) \quad (2.4)$$

with $\tilde{P}^2 = \max(P^2, \mu^2)$ and $\eta(P^2) = (1 + P^2/m_\rho^2)^{-2}$ where $m_\rho^2 = 0.59\text{GeV}^2$ refers to some effective mass in the vector-meson propagator; furthermore

$$f_{\text{non-pert}}^{\gamma(P^2)}(x, \tilde{P}^2) = \kappa (4\pi\alpha/f_\rho^2) \begin{cases} f^\pi(x, P^2) & , \quad P^2 > \mu^2 \\ f^\pi(x, \mu^2) & , \quad 0 \leq P^2 \leq \mu^2 \end{cases} \quad (2.5)$$

and

$$\begin{aligned} q_{pert}^{\gamma(P^2)}(x, \tilde{P}^2) &= \bar{q}_{pert}^{\gamma(P^2)}(x, \tilde{P}^2) = \begin{cases} 0, & \text{LO} \\ 3e_q^2 \frac{\alpha}{2\pi} \left[(x^2 + (1-x)^2) \ln \frac{1}{x^2} - 2 + 6x - 6x^2 \right], & \text{NLO} \end{cases} \\ g_{pert}^{\gamma(P^2)}(x, \tilde{P}^2) &= 0 \end{aligned} \quad (2.6)$$

where the NLO boundary conditions are again specified in the DIS_γ factorization scheme and $\mu_{LO}^2 = 0.25 \text{ GeV}^2$ and $\mu_{NLO}^2 = 0.3 \text{ GeV}^2$ refer to the LO and NLO input scales for the parton distributions of the real photon. The boundary conditions (2.5) and (2.6) apply both in LO and NLO. The resulting LO distributions at $Q^2 \geq \tilde{P}^2$ are presented in the Appendix and are applicable at $Q^2 \gg P^2$ where higher twist $(P^2/Q^2)^n$ contributions are likely to be negligible and transverse photon contributions dominate.

3 Heavy Quark Electroproduction

The cross section for heavy quark ($h = c, b, \dots$) electroproduction is given by

$$\frac{d\sigma_{ep}^h}{dP^2 dy} = \frac{2\pi\alpha^2}{(P^2)^2 y} \left[(1 + (1-y)^2) F_2^h(x, P^2) - y^2 F_L^h(x, P^2) \right] \quad (3.1)$$

with $x = P^2/sy$ and where the 'direct' contribution to $F_{2,L}^h$ arise in LO from $\gamma(P^2)g \rightarrow h\bar{h}$,

$$\frac{1}{x} F_{2,L}^h(x, P^2) = 2e_h^2 \frac{\alpha_s(\mu_F^2)}{2\pi} \int_{ax}^1 \frac{dx'}{x'} C_{2,L} \left(\frac{x}{x'}, \rho \right) g(x', \mu_F^2) \quad (3.2)$$

with

$$\begin{aligned} C_2(z, \rho) &= \frac{1}{2} \left\{ \left[z^2 + (1-z)^2 + z(1-3z)\rho - \frac{1}{2}z^2\rho^2 \right] \ln \frac{1+\beta}{1-\beta} \right. \\ &\quad \left. + \beta [-1 + 8z(1-z) - z(1-z)\rho] \right\} \end{aligned} \quad (3.3)$$

$$C_L(z, \rho) = -z^2\rho \ln \frac{1+\beta}{1-\beta} + 2\beta z(1-z) \quad (3.4)$$

where $\rho \equiv 4m_h^2/P^2$, $a = 1 + \rho$, $\beta^2 = 1 - \rho z(1-z)^{-1}$ and the factorization scale μ_F should be preferably chosen at $\mu_F^2 = 4m_h^2$, irrespective of P^2 , which results in a satisfactory perturbative stability when compared with the appropriate NLO contribution [7]. The

description of the above 'direct' heavy quark electroproduction in terms of $\sigma_{\gamma p}^h$ for the process $\gamma p \rightarrow h\bar{h}$ with γ denoting an effective, transversely polarized, massless photon, $\gamma \equiv \gamma(P^2 = 0)$, yields the approximation [8]

$$\frac{d\sigma_{ep}^h}{dP^2 dy} \simeq \frac{\alpha}{2\pi} \frac{1}{P^2} \frac{1 + (1-y)^2}{y} \sigma_{\gamma p}^h(sy) \quad (3.5)$$

where

$$\sigma_{\gamma p}^h(sy) = \frac{1}{sy} \int_{4m_h^2}^{sy} d\hat{s} \, g\left(\frac{\hat{s}}{sy}, \mu_F^2\right) \hat{\sigma}_{\gamma g}^h(\hat{s}) \quad , \quad (3.6)$$

with the cross section for the 'direct' subprocess $\gamma g \rightarrow h\bar{h}$ being given by

$$\hat{\sigma}_{\gamma g}^h(\hat{s}) = e_h^2 \frac{2\pi\alpha\alpha_s(\mu_F^2)}{\hat{s}} \left[\frac{1}{2}(3 - \hat{\beta}^4) \ln \frac{1 + \hat{\beta}}{1 - \hat{\beta}} - \hat{\beta}(2 - \hat{\beta}^2) \right] \quad (3.7)$$

where $\hat{\beta}^2 = 1 - 4m_h^2/\hat{s}$. The validity of this approximation determines the allowed range in P^2 where the virtual photon concept, in the sense discussed in [1-3], is meaningful. We recall that our expectations concerning this issue are that as long as $P^2 \ll \mu_F^2 \simeq 4m_h^2$ is fulfilled, the effective virtual photon concept is useful and the study of its partonic content applicable to investigations concerning the so called 'resolved photon' contributions. In fact we find that as long as $P^2/\mu_F^2 \lesssim 10^{-1}$ the effective virtual photon approximation, Eq.(3.5), reproduces the results of the exact calculation, Eq.(3.1), at a level of up to about 10% accuracy. This is illustrated in Tables 1 and 2 for charm and bottom production, respectively, where we used $\mu_F^2 = 4m_h^2$ together with $m_c = 1.5 \text{ GeV}$ and $m_b = 4.5 \text{ GeV}$. [Note that, for a given P^2 , the validity of the approximation (3.5) is almost independent of y due to the smallness of F_L^h in (3.1)]. We thus expect that in general the effective photon concept is reasonably applicable whenever $P^2 \lesssim 10^{-1}\mu_F^2$ and that its resolved parton content is discernible provided it contributes significantly more than 10% to the involved production rate. This latter requirement is necessary also due to additional uncertainties related to different choices of the factorization scale (e.g., $\mu_F^2 = m_h^2$) and to the size of NLO corrections [1, 7]. As shown in Figs. 1 and 2, these conditions are almost never satisfied for heavy quark (c , b) electroproduction where the resolved contribution, to be added to the direct $\sigma_{\gamma p}^h$ in (3.5), is given by [9]

$$\sigma_{\gamma p, res}^h(s_{\gamma^* p}) = \sum_{f\gamma} \sum_f \int dx_\gamma dx \, f^{\gamma(P^2)}(x_\gamma, \mu_F^2) f(x, \mu_F^2) \hat{\sigma}^{f\gamma f}(x_\gamma x s_{\gamma^* p}, m_h^2, \mu_F^2) \quad (3.8)$$

with $s_{\gamma^*p} = ys - P^2$. The dominant LO hadronic $2 \rightarrow 2$ (as well as NLO $2 \rightarrow 3$) subprocess cross sections $\hat{\sigma}^{f\gamma f}$ for $h\bar{h}$ production, i.e., $f\gamma f \rightarrow h\bar{h}$ etc. with $f = q, \bar{q}, g$, are well known [9]. Due to the smallness of the hadronic 'resolved' contributions for $P^2 \equiv Q^2 \neq 0$ in Figs. 1 and 2, electroproduction of heavy quarks appears to be unsuitable for studies of the resolved parton content of the virtual photon at HERA - *unless* one can tag experimentally on the resolved contribution via the *hadronic photon remnants*. The situation here is not too different from that for real photons [9], $P^2 = 0$, and improves for LEP * LHC ($\sqrt{s} \simeq 1265 \text{ GeV}$). For $h = b$ (Fig. 2) a P^2 dependence of the resolved component may be discernible for $P^2 < 1 \text{ GeV}^2$ where the effective photon description is accurate at a level of 1% (Table 2) and the resolved component's contribution is about or exceeds 10%.

On the other hand, the smallness of the resolved contribution of virtual ($P^2 \equiv Q^2 > 0$) photons to heavy quark production implies that ep scattering at HERA allows for reliable predictions of heavy quark production rates uncontaminated by the resolved contributions. Finally it should be noted that photoproduction ($P^2 = 0$) of charm, $\gamma p \rightarrow c\bar{c}X$, has already been measured at HERA [11, 12] and first preliminary measurements for electroproduction ($P^2 > 0$) of charm, $ep \rightarrow e c\bar{c}X$, i.e, for $F_2^c(x, P^2 \equiv Q^2)$ have recently appeared [13].

4 Jet Electroproduction

Turning now to high- E_T single-inclusive jet production, $ep \rightarrow jet + X$, we shall study the P^2 dependence of the resolved photon contribution in the range $P^2 \lesssim 10^{-1} \mu_F^2$ indicated in the previous section as suitable for an effective photon description. It now turns out that in large kinematical regions the resolved photon contribution to the jet production rate is indeed significant and thus allows for a reliable study of its P^2 dependence. For definiteness we shall study $d\sigma_{ep}^{jet}/dP^2 dE_T dy d\eta_{lab}$ at the HERA ep collider with realistic values chosen for E_T , y and η_{lab} , where $d\sigma_{ep}^{jet}$ replaces $d\sigma_{ep}^h$ in (3.5) and similarly $\sigma_{\gamma p}^h$ is

replaced by the direct and resolved contributions

$$\begin{aligned}
d\sigma_{\gamma p}^{jet} &= d\sigma_{dir}^{jet} + d\sigma_{res}^{jet} \\
&= \sum_{f=q,\bar{q},g} \int dx f(x, \mu_F^2) d\hat{\sigma}_{\gamma f}^{jet} \\
&+ \sum_{f\gamma} \sum_f \int dx_\gamma dx f^{\gamma(P^2)}(x_\gamma, \mu_F^2) f(x, \mu_F^2) d\hat{\sigma}_{f\gamma f}^{jet} \quad .
\end{aligned} \tag{4.1}$$

The LO $\gamma f \rightarrow q\bar{q}$ and hadronic $2 \rightarrow 2$ subprocess cross sections $d\hat{\sigma}_{\gamma f}^{jet}$ and $d\hat{\sigma}_{f\gamma f}^{jet}$, respectively, can be found, for example, in [14]. The charmed quark jet's contribution is included via $\gamma g \rightarrow c\bar{c}$ in the 'direct' channel and in the 'resolved' channel via $g^{\gamma(P^2)}g \rightarrow c\bar{c}$, etc., with the relevant unintegrated matrix elements being given in [15] and [16], respectively. The sensitivity to the actual value of m_c is small due to $m_c^2/E_T^2 \ll 1$ for typically chosen values of E_T . The chosen E_T of the jet for realistic experiments should not be too small for several obvious reasons: (i) The jet should be clearly separable from possible beam contaminations, (ii) $P^2 \lesssim 10^{-1}E_T^2$ should be fulfilled over a wide range of P^2 and (iii) perturbative calculations of its production rate should be reliable. On the other hand E_T should not be too large in order that (i) a reasonable signal is still available and (ii) the resolved contribution is still significant. The choice $E_T \gtrsim 5 - 7 \text{ GeV}$ and consequently $\mu_F \sim E_T$, as also employed by recent experimental analyses of photoproduced single-jet [17] and dijet [18] events, seems to meet all these requirements. As for y we will choose $y \simeq 0.5$ as representative for the realistic range $0.2 \lesssim y \lesssim 0.8$ containing a sufficient flux of energetic photons. Finally, the pseudorapidity η_{lab} in the HERA lab-frame should be chosen so as to guarantee a significant contribution of the resolved partons to $d\sigma^{jet}$ over a wide range of P^2 . This happens for [19] $-1 \lesssim \eta_{lab} \lesssim 2.5$. We shall evaluate the resulting relevant ratio [cf. Eq.(4.1)]

$$\left(\frac{res}{dir}\right)^{jet} \equiv d\sigma_{res}^{jet}(P^2; E_T, y, \eta_{lab})/d\sigma_{dir}^{jet}(P^2; E_T, y, \eta_{lab}) \tag{4.2}$$

for the above specified values of E_T , y and η_{lab} . This ratio will be analysed in LO since NLO corrections are expected to be less significant in the above ratio. Moreover the NLO/LO stability for photoproduction ($P^2 = 0$) of jets has been demonstrated [20, 21]

as well as the stability with respect to the choice of the renormalization and factorization scale $\mu_F \simeq E_T$. Most of our quantitative results are based on using in Eq.(4.1) the LO parton distributions of the proton in [10] and of the virtual photon in [1], unless stated otherwise.

The result of our numerical calculations are shown in Figs. 3-5 as a function of P^2 for various fixed values of E_T and η_{lab} at a typical average $y \simeq 0.5$. These demonstrate clearly the feasibility of investigating the P^2 dependent parton distributions of the virtual photon at HERA, in particular of course in the forward (proton) beam direction $\eta_{lab} > 0$ (i.e. small x_γ), up to $P^2 \simeq 5 \text{ GeV}^2$, i.e., up to $P^2/E_T^2 \simeq 10^{-1}$, where the effective virtual photon concept is still meaningful. It is interesting to note that even for $\eta_{lab} \leq 0$ (large(r) x_γ), the resolved component is still comparable to the direct one, i.e., $res/dir \lesssim 3$ as shown in Fig. 4. This implies that jet production in ep collisions by virtual ($P^2 \equiv Q^2 \neq 0$) photons at HERA energies rarely proceeds via the 'direct' γ^* -contribution alone, since the resolved components of the virtual photon remain effective for $-1 \lesssim \eta_{lab} \lesssim 2.5$ at the relevant E_T and P^2 . It should be mentioned that preliminary results [22] on the integrated event-rate for dijet production in ep collisions with virtual ($0.1 < P^2 < 0.55 \text{ GeV}^2$) photons have recently demonstrated the relevance of their resolved components.

Finally, in Fig. 6 we compare our results with those obtained utilizing the parton distributions of the virtual photon in [2]: SaS 1D and SaS 2D refer to rather different virtual photon parton densities, corresponding to evolution input scales $Q_0^2 = 0.36 \text{ GeV}^2$ and 4 GeV^2 , respectively, from where appropriately modified VMD inputs are evolved. The predicted P^2 dependence of ' res/dir ' in Fig. 6 is not too different from the one based on the GRS parton distributions [1] of the virtual photon. Similar results hold for other values of E_T and η_{lab} considered previously.

5 Summary and Conclusions

Parton densities of virtual ($P^2 \neq 0$) photons can be rather uniquely calculated in LO and NLO QCD which, moreover, extrapolate smoothly to $P^2 = 0$, i.e., to the hadronic 'resolved' structure functions of a real photon [1]. The virtual photon structure function $F_2^{\gamma(P^2)}(x, Q^2)$ can be measured via the subprocess $\gamma^*(Q^2)\gamma(P^2) \rightarrow X$ in $e^+e^- \rightarrow e^+e^-X$ at LEP2 [23] or in tagged $ep \rightarrow eX$ collisions at DESY-HERA via the subprocess $\gamma(P^2)p \rightarrow X$ where the parton densities $f^{\gamma(P^2)}(x, \mu_F^2)$, $f = q, \bar{q}, g$ and $P^2 \equiv Q^2$, describe the 'resolved' hadronic component of the virtual photon $\gamma^* \equiv \gamma(P^2)$.

Here we have shown that the predicted [1-2] P^2 dependence of the parton distributions $f^{\gamma(P^2)}$ inside the virtual photon may be tested at the DESY-HERA ep collider via tagged measurements of single jet or $b\bar{b}$ pair production. In particular the observation of single jets with transverse energy $E_T^{jet} \simeq 5 - 7 \text{ GeV}$ and pseudorapidity $\eta_{lab} > 0$ will provide for a reliable determination of $f^{\gamma(P^2)}(x_\gamma, E_T^2)$ at $P^2 \lesssim 5 \text{ GeV}^2$. For $\eta_{lab} \leq 0$, where larger values of x_γ are probed, the contributions due to the 'resolved' components $f^{\gamma(P^2)}(x_\gamma, E_T^2)$ are still comparable to the 'direct' contribution from the unresolved $\gamma(P^2)$.

A determination of $g^{\gamma(P^2)}(x_\gamma, 4m_b^2)$ is shown to be feasible at $P^2 \lesssim 1 \text{ GeV}^2$ where the resolved contribution to $d\sigma(ep \rightarrow e b\bar{b}X)$ amounts to about 10%. As a byproduct we note that all the delineated kinematical regions where the resolved contributions due to $f^{\gamma(P^2)}$ are negligible, such as for example in $c\bar{c}$ production, are particularly suitable for a reliable determination of parton distributions inside the proton: Most important is the possibility of fixing $g(x, 4m_c^2)$ via $ep \rightarrow e c\bar{c}X$ at all conceivable values of P^2 . Furthermore, $g^{\gamma(P^2)}(x_\gamma, 4m_c^2)$ can be determined even in the aforementioned $ep \rightarrow e c\bar{c}X$ process *provided* the *hadronic remnants* of the photon can be detected experimentally. A similar remark obviously pertains also for jet events, in particular for those with $\eta_{lab} < 0$ relevant for the larger- x_γ region.

Finally it should be stressed again that, according to our analysis in Sec. 3, the concept

of a resolved virtual photon is only meaningful for virtualities constrained by $P^2 \lesssim 10^{-1} \mu_F^2$ with μ_F^2 denoting the typical momentum scale of the underlying hard processes.

Acknowledgement

This work has been supported in part by the 'Bundesministerium für Bildung, Wissenschaft, Forschung und Technologie', Bonn.

Appendix

In order to obtain parametrizations of our radiative (dynamical) LO predictions [1] for the parton densities $f^{\gamma(P^2)}(x, Q^2)$ of the virtual photon $\gamma(P^2)$, valid for $Q^2 > \mu_{LO}^2 = 0.25 \text{ GeV}^2$, we write

$$x f^{\gamma(P^2)}(x, Q^2) = x f_{PL}^{\gamma(P^2)}(x, Q^2) + x f_{HAD}^{\gamma(P^2)}(x, Q^2) \quad . \quad (\text{A1})$$

The pointlike (PL) contributions [1] are parametrized as ($\alpha = 1/137$)

$$x f_{PL}^{\gamma(P^2)}(x, Q^2)/\alpha = \left[s x^a (A + B\sqrt{x} + Cx^b) + s^\alpha e^{-E + \sqrt{E'} s^\beta \ln \frac{1}{x}} \right] (1-x)^D \quad (\text{A2})$$

where

$$s = \ln \frac{\ln(Q^2/(0.232 \text{ GeV})^2)}{\ln(\tilde{P}^2/(0.232 \text{ GeV})^2)} \quad (\text{A3})$$

with $\tilde{P}^2 = \max(P^2, \mu_{LO}^2)$. The Q^2 dependence of the quantities a, b, A, B, \dots is described as usual in terms of power series in s , as defined in Table 3, with coefficients F, G, H which in turn are, according to Table 3, expanded as, e.g.

$$G = g_1 + g_2 l_1(P^2) + g_3 l_2(P^2) \quad (\text{A4})$$

in order to describe the P^2 dependence in (A2), with

$$l_1(P^2) = \ln^2(\tilde{P}^2/\mu_{LO}^2) \quad , \quad l_2(P^2) = \ln \left[\tilde{P}^2/\mu_{LO}^2 + \ln(\tilde{P}^2/\mu_{LO}^2) \right] \quad . \quad (\text{A5})$$

All the required constants are tabulated in Table 3 for the pointlike $u = \bar{u}$, $d = \bar{d} = s = \bar{s}$ and g densities (A2).

The hadronic (HAD) contributions to (A1), being generated from the VMD-like boundary conditions [1], are parametrized as

$$xf_{HAD}^{\gamma(P^2)}(x, Q^2)/\alpha = \eta(P^2) \left[x^a (A + B\sqrt{x} + Cx^b) + s^\alpha e^{-E + \sqrt{E' s^\beta \ln \frac{1}{x}}} \right] (1-x)^D \quad (\text{A6})$$

for the hadronic $u = \bar{u} = d = \bar{d}$ and g densities, and as

$$xs_{HAD}^{\gamma(P^2)}(x, Q^2)/\alpha = \eta(P^2) \left[s x^a (A + B\sqrt{x} + Cx^b) + s^\alpha e^{-E + \sqrt{E' s^\beta \ln \frac{1}{x}}} \right] (1-x)^D \quad (\text{A7})$$

for the $s = \bar{s}$ density, with $\eta(P^2) = (1 + P^2/m_\rho^2)^{-2}$ and $m_\rho^2 = 0.59 \text{ GeV}^2$. The Q^2 dependence of (A6) and (A7) is described by expanding again a, b, A, B, \dots in terms of

$$s = \ln \frac{\ln(Q^2/(0.232 \text{ GeV})^2)}{\ln(\mu_{LO}^2/(0.232 \text{ GeV})^2)} \quad (\text{A8})$$

as described in Table 4.

All above parametrizations are valid for

$$\begin{aligned} P^2 &\leq 10 \text{ GeV}^2, \quad 10^{-4} \leq x \leq 1 \\ 0.6 \leq Q^2 &\leq 5 \times 10^4 \text{ GeV}^2 \quad \underline{\text{and}} \quad Q^2 \gtrsim 5P^2 \end{aligned} \quad (\text{A9})$$

and are obtainable as a FORTRAN package via electronic mail from strat@hal1.physik.uni-dortmund.de

References

- [1] M. Glück, E. Reya and M. Stratmann, Phys. Rev. D51, 3220 (1995).
- [2] G.A. Schuler and T. Sjöstrand, Z. Phys. C68, 607 (1995); CERN-TH/96-04.
- [3] B.L. Ioffe and A. Oganesian, Z. Phys. C69, 119 (1995).
- [4] M. Glück, E. Reya and A. Vogt, Phys. Rev. D46, 1973 (1992).
- [5] M. Glück, E. Reya and A. Vogt, Z. Phys. C53, 651 (1992).
- [6] M. Glück, E. Reya and A. Vogt, Phys. Rev. D45, 3986 (1992).
- [7] M. Glück, E. Reya and M. Stratmann, Nucl. Phys. B422, 37 (1994).
- [8] V.M. Budnev, I.F. Ginzburg, G.V. Meledin and V.G. Serbo, Phys. Rep. 15, 181 (1975);
S. Frixione, M.L. Mangano, P. Nason and G. Ridolfi, Phys. Lett. B319, 339 (1993).
- [9] M. Glück, E. Reya and A. Vogt, Phys. Lett. B285, 285 (1992) and references therein.
- [10] M. Glück, E. Reya and A. Vogt, Z. Phys. C67, 433 (1995).
- [11] M. Derrick et al., ZEUS collab., Phys. Lett. B349, 225 (1995);
S. Aid et al., H1 collab., DESY 96-55.
- [12] For a recent comparative review see, for example, A.C. Caldwell, DESY 95-231 (to appear in the Proceedings of the XVIIth Int. Symposium on Lepton-Photon Interactions, Beijing, China, August 1995).
- [13] A. de Roeck, H1 collab., plenary talk presented at the Cracow Epiphany Conference on the Proton Structure, Cracow, Poland, January 1996 (to appear in the Proceedings); H1 collab., contributed paper EPS-0785 to the Int. Europhysics Conf. on High Energy Physics, Brussels, 1995.

- [14] V.D. Barger and R.J.N. Phillips, 'Collider Physics' (Addison - Wesley Pub., 1987), pp. 296;
R. Gastmans and T.T. Wu, 'The Ubiquitous Photon' (Oxford Science Pub., 1990), pp. 385.
- [15] L.M. Jones and H.W. Wyld, Phys. Rev. D17, 759 (1978).
- [16] M. Glück, J.F. Owens and E. Reya, Phys. Rev. D17, 2324 (1978).
- [17] I. Abt et al., H1 collab, Phys. Lett. B314, 436 (1993);
M. Derrick et al., ZEUS collab., Phys. Lett. B322, 287 (1994) and B342, 417 (1995).
- [18] T. Ahmed et al., H1 collab, Nucl. Phys. B445, 195 (1995);
M. Derrick et al., ZEUS collab., Phys. Lett. B348, 665 (1995); and B354, 163 (1995).
- [19] Higher values of η_{lab} should be avoided in order to guarantee clean jets, uncontaminated by the beam region.
- [20] G. Kramer and S.G. Salesch, Z. Phys. C61, 277 (1994);
M. Klasen, G. Kramer and S.G. Salesch, Z. Phys. C68, 113 (1995);
S.G. Salesch, DESY 93-196 (Ph.D. thesis, 1993).
- [21] P. Aurenche, J.-Ph. Guillet and M. Fontannaz, Phys. Lett. B338, 98 (1994).
- [22] M.L. Utley, ZEUS collab., Univ. Glasgow report GLAS-PPE/95-03, talk presented at the Int. Europhysics Conf. on High Energy Physics, Brussels, 1995 (to appear in the proceedings).
- [23] P. Aurenche and G.A. Schuler (conveners) et al., in 'Physics at LEP2', CERN 96-01, vol.1, p.291.

Tables

Table 1. Cross sections for direct electroproduction of charm ($m_c = 1.5 \text{ GeV}$) at HERA energies $\sqrt{s} = 298 \text{ GeV}$ for various photon virtualities P^2 and energy fractions y . The exact results refer to Eqs. (3.1)-(3.4) and the approximate ones to Eqs. (3.5)-(3.7), with the percental differences being shown in the last column.

P^2/GeV^2	y	EXACT (nb)	APPROX (nb)	%
0.2	0.1	369.2	378.5	2.52
	0.5	108.4	111.1	2.49
	0.7	77.98	80.02	2.62
0.5	0.1	142.4	151.4	6.32
	0.5	41.80	44.43	6.29
	0.7	30.02	32.01	6.63
1.0	0.1	67.09	75.70	12.8
	0.5	19.71	22.22	12.7
	0.7	14.12	16.00	13.3

Table 2. As in Table 1 but for bottom production ($m_b = 4.5 \text{ GeV}$).

P^2/GeV^2	y	EXACT (nb)	APPROX (nb)	%
0.5	0.1	0.962	0.970	0.83
	0.5	0.404	0.407	0.74
	0.7	0.308	0.311	0.97
2.0	0.1	0.234	0.243	3.85
	0.5	0.099	0.102	3.03
	0.7	0.075	0.078	4.00
5.0	0.1	0.089	0.097	8.99
	0.5	0.038	0.041	7.89
	0.7	0.029	0.031	6.90
10.0	0.1	0.041	0.0485	18.29
	0.5	0.0175	0.0204	16.57
	0.7	0.0133	0.0155	16.54

Table 3 Expansion parameters for the parametrizations of the pointlike (PL) contribution to (A1), according to Eqs. (A2)-(A5).

	u								
	$F = f_1 + f_2 l_1(P^2) + f_3 l_2(P^2)$			$G = g_1 + g_2 l_1(P^2) + g_3 l_2(P^2)$			$H = h_1 + h_2 l_1(P^2) + h_3 l_2(P^2)$		
	f_1	f_2	f_3	g_1	g_2	g_3	h_1	h_2	h_3
$\alpha = F$	1.551	-0.139	0.783	-	-	-	-	-	-
$\beta = F$	0.105	0.132	0.087	-	-	-	-	-	-
$a = F + G \cdot s$	1.089	0.003	-0.0134	-0.172	0.009	-0.017	-	-	-
$b = F + G \sqrt{s} + H s^2$	3.822	0.092	-0.516	-2.162	-0.085	0.439	0.533	0.013	0.108
$A = F + G \sqrt{s}$	0.377	-0.013	0.27	0.299	0.107	-0.097	-	-	-
$B = F + G s + H s^2$	-0.467	-0.019	-0.272	-0.412	-0.167	0.138	0.2	0.076	0.026
$C = F + G s$	0.487	0.04	0.124	0.0766	0.064	-0.016	-	-	-
$D = F + G s$	0.119	0.011	-0.065	0.063	0.002	0.044	-	-	-
$E = F + G s$	7.605	0.057	-1.009	0.234	-0.057	0.622	-	-	-
$E' = F + G s$	-0.567	0.162	0.227	2.294	-0.172	-0.184	-	-	-

	$d = s$								
	$F = f_1 + f_2 l_1(P^2) + f_3 l_2(P^2)$			$G = g_1 + g_2 l_1(P^2) + g_3 l_2(P^2)$			$H = h_1 + h_2 l_1(P^2) + h_3 l_2(P^2)$		
	f_1	f_2	f_3	g_1	g_2	g_3	h_1	h_2	h_3
$\alpha = F$	2.484	0.033	0.007	-	-	-	-	-	-
$\beta = F$	1.214	-0.0516	0.12	-	-	-	-	-	-
$a = F + G s$	1.088	0.001	-0.013	-0.1735	0.018	-0.028	-	-	-
$b = F + G \sqrt{s} + H s^2$	4.293	0.102	-0.595	-2.802	-0.114	0.669	0.5975	0.022	0.001
$A = F + G s$	0.128	0.004	0.054	0.0337	0.025	-0.02	-	-	-
$B = F + G s + H s^2$	-0.1193	-0.003	-0.0583	-0.0872	-0.041	0.035	0.0418	0.009	0.009
$C = F + G s$	0.127	0.007	0.032	0.0135	0.021	-0.009	-	-	-
$D = F + G s$	0.14	0.01	-0.06	0.0423	0.004	0.036	-	-	-
$E = F + G s$	6.946	-0.067	-0.39	0.814	0.06	0.033	-	-	-
$E' = F + G s$	1.531	-0.148	0.245	0.124	0.13	-0.171	-	-	-

	g								
	$F = f_1 + f_2 l_1(P^2) + f_3 l_2(P^2)$			$G = g_1 + g_2 l_1(P^2) + g_3 l_2(P^2)$			$H = h_1 + h_2 l_1(P^2) + h_3 l_2(P^2)$		
	f_1	f_2	f_3	g_1	g_2	g_3	h_1	h_2	h_3
$\alpha = F$	1.682	0.025	-	-	-	-	-	-	-
$\beta = F$	1.1	-0.018	0.112	-	-	-	-	-	-
$a = F + G \sqrt{s}$	0.5888	-0.025	0.177	-0.4714	-0.022	0.024	-	-	-
$b = F + G s^2$	0.5362	0.001	-0.0104	0.0127	-	-	-	-	-
$A = F + G \sqrt{s} + H s^2$	0.07825	0.0	0.053	0.05842	0.005	-0.058	0.08393	0.034	0.073
$B = F + G s$	-2.438	-1.082	-1.666	0.03399	0.0	0.086	-	-	-
$C = F + G s^2$	2.348	1.08	1.63	-0.07182	-0.0256	-0.088	-	-	-
$D = F + G s + H s^2$	1.084	-	-	0.3098	-0.004	0.016	-0.07514	0.007	-0.012
$E = F + G s$	3.327	0.01	-0.673	1.1	0.126	-0.167	-	-	-
$E' = F + G s$	2.264	0.032	-0.227	0.2675	0.086	-0.159	-	-	-

Table 4 Expansion parameters for the parametrizations of the hadronic (HAD) contribution to (A1), according to Eqs. (A6)-(A8).

	$u = d$			s			g		
	F	G	H	F	G	H	F	G	H
$\alpha = F$	0.756	-	-	0.902	-	-	0.364	-	-
$\beta = F$	0.187	-	-	0.182	-	-	1.31	-	-
$a = F + G\sqrt{s} + Hs$	0.109	-	-0.163	0.271	-	-0.346	0.86	-0.254	-
$b = F + Gs + Hs^2$	22.53	-21.02	5.608	17.1	-13.29	6.519	0.611	-	0.008
$A = F + G\sqrt{s} + Hs^2$	0.002	0.004	-	0.017	-0.01	-	-0.843	2.248	-0.201
$B = F + Gs + Hs^2$	0.332	-0.008	-0.021	0.031	-0.0176	0.003	-0.097	-2.412	
$C = F + Gs + Hs^2$	0.054	-0.039	-	-0.011	0.0065	-	1.33	-	0.572
$D = F + Gs + Hs^2$	0.381	0.572	-	1.243	0.804	-	0.44	1.233	0.009
$E = F + Gs$	4.774	1.436	-	4.709	1.499	-	0.954	1.862	-
$E' = F + Gs$	-0.614	3.548	-	-0.48	3.401	-	3.791	-0.079	-

Figure Captions

Fig. 1 The ratio of the 'resolved' [Eq.(3.8)] to the 'direct' [Eq.(3.6)] contribution to charm production in LO-QCD for various fixed values of P^2 (in GeV^2 units), using $m_c = 1.5 \text{ GeV}$ and $\mu_F^2 = 4m_c^2$. The GRV 94 parton densities of the proton are taken from [10] and the ones of the virtual photon from [1]. For comparison the total ep (dir.+res.) charm production rate at HERA for $P^2 = 0$ is about $0.5 \mu\text{b}$ [9] at $\sqrt{s} \simeq 300 \text{ GeV}$.

Fig. 2 As in Fig. 1 but for bottom production, using $m_b = 4.5 \text{ GeV}$ and $\mu_F^2 = 4m_b^2$. The total ep (dir.+res.) bottom production rate at HERA for $P^2 = 0$ is about 6 nb [9] at $\sqrt{s} \simeq 300 \text{ GeV}$.

Fig. 3 The ratio of the 'resolved' to the 'direct' contribution, defined in Eq.(4.2), for inclusive single jet production in LO-QCD in ep collisions at $\sqrt{s} = 298 \text{ GeV}$ as a function of P^2 . The LO parton densities of the virtual photon are from [1] and the ones of the proton are taken from [10]. Furthermore $\mu_F^2 = E_T^2$.

Fig. 4 As in Fig. 3 but for $\eta_{lab} \leq 0$.

Fig. 5 As in Fig. 3 but for different values of E_T at fixed $\eta_{lab} = 1.5$.

Fig. 6 Comparison of our results in Fig. 3 at $\eta_{lab} = 1.5$ with the predictions due to two other representative sets [2] of parton densities of the virtual photon.

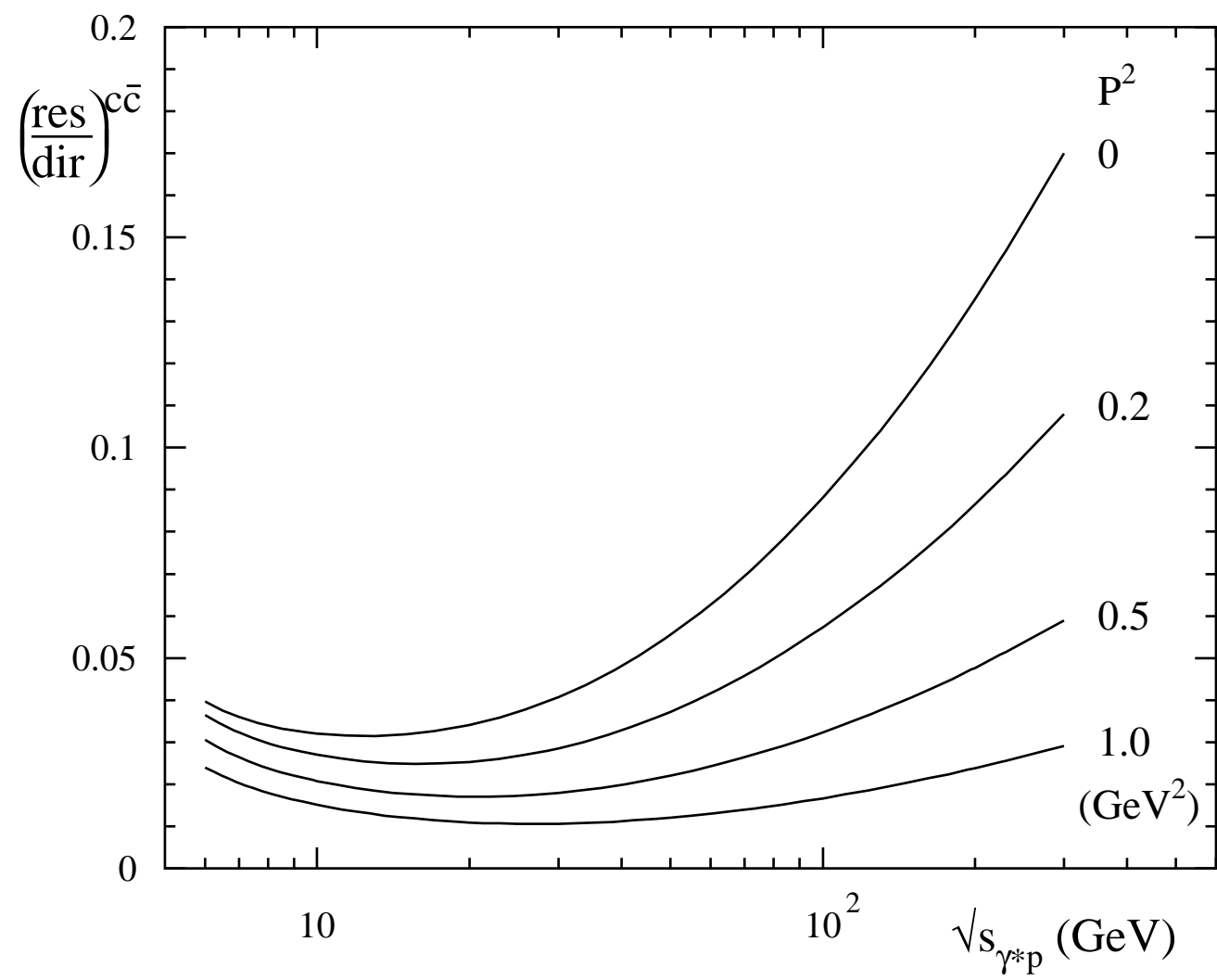


Fig. 1

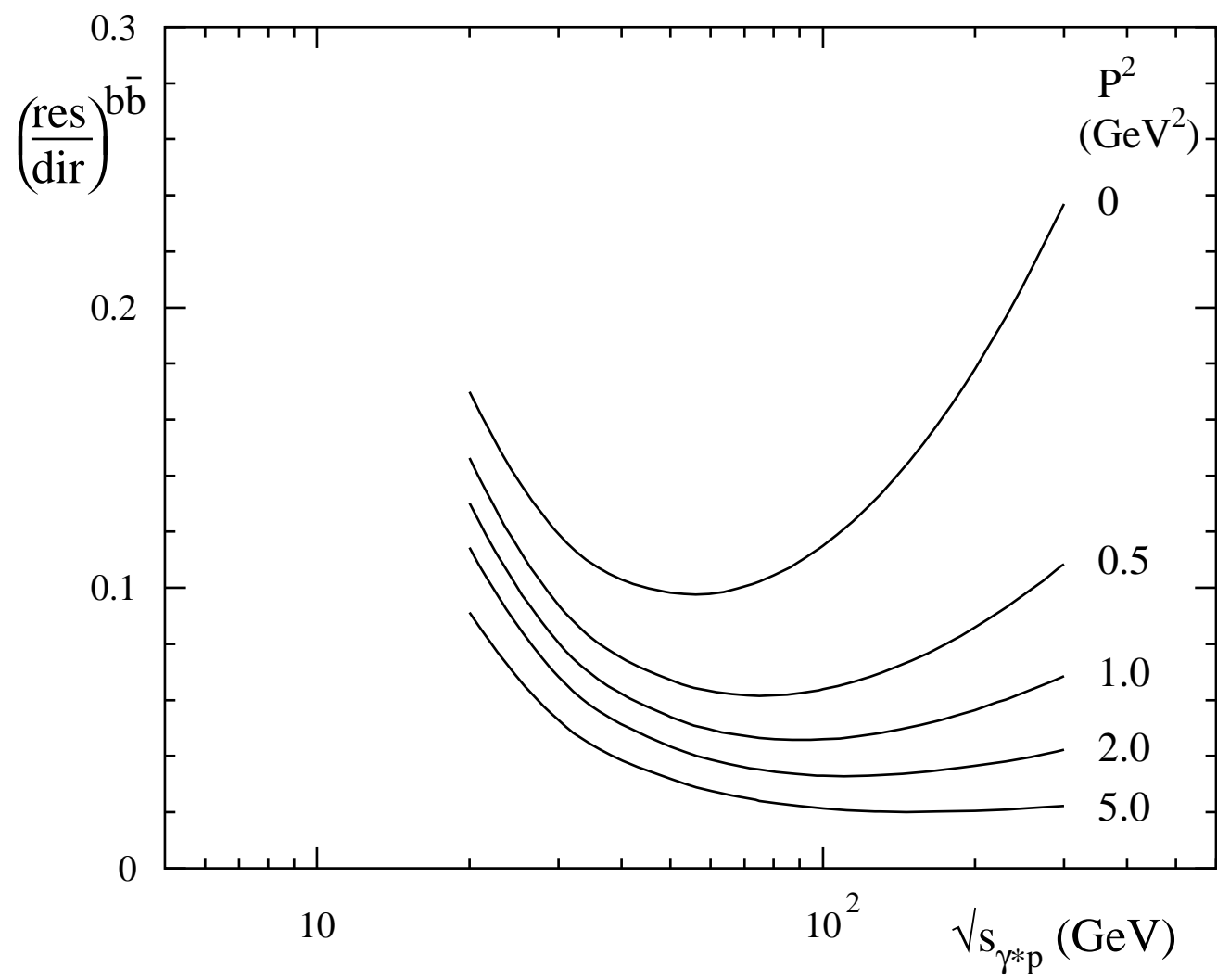


Fig. 2

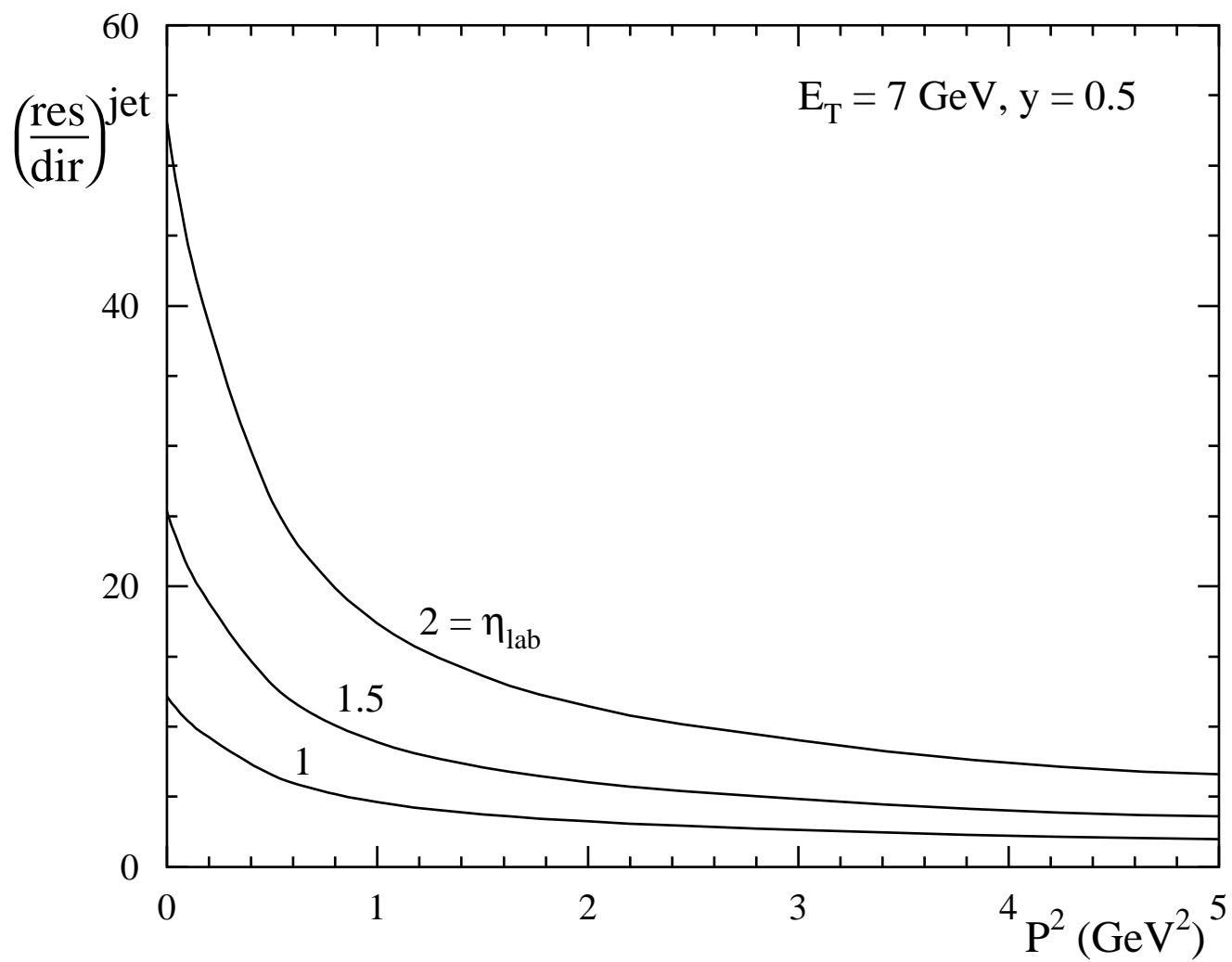


Fig. 3

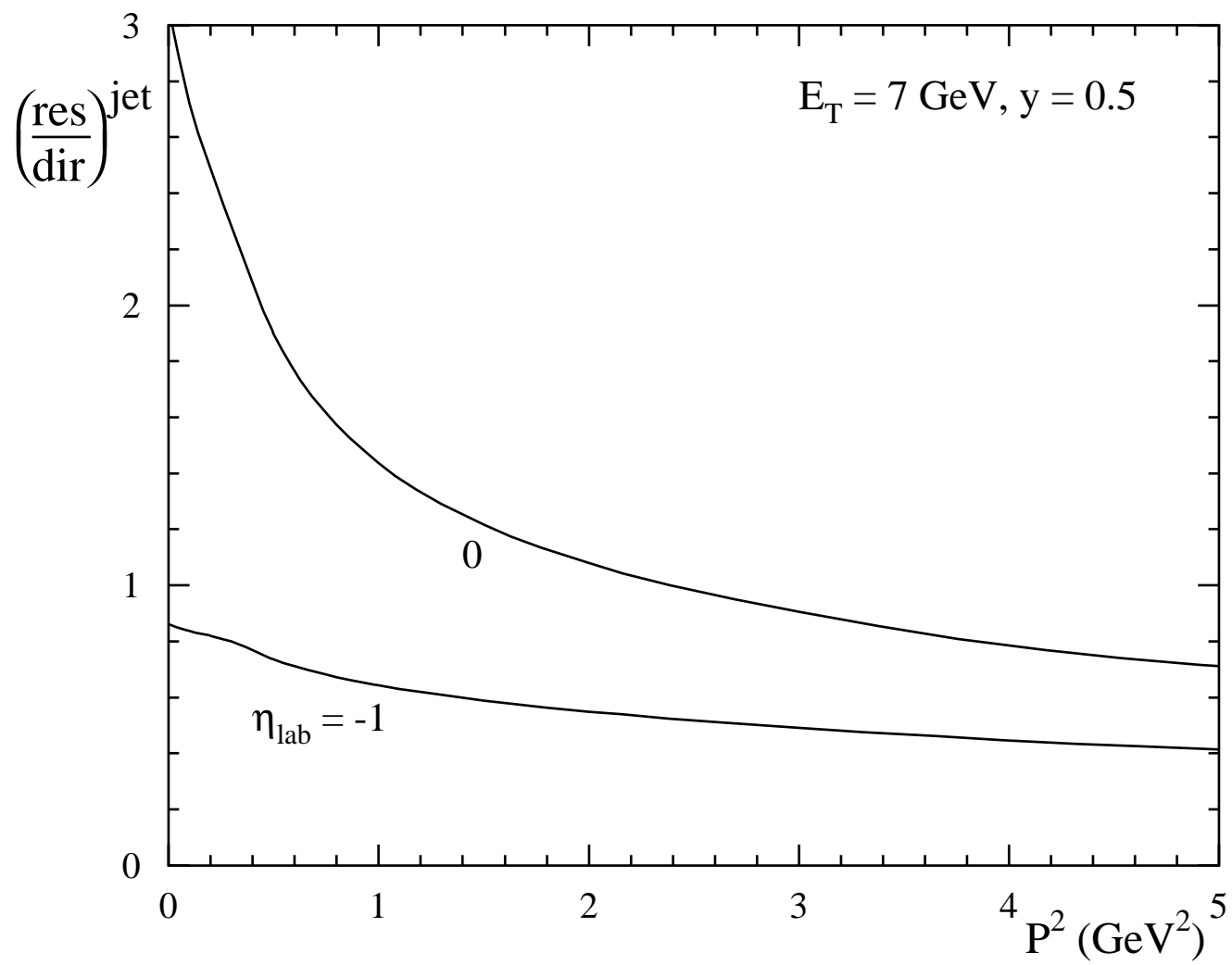


Fig. 4

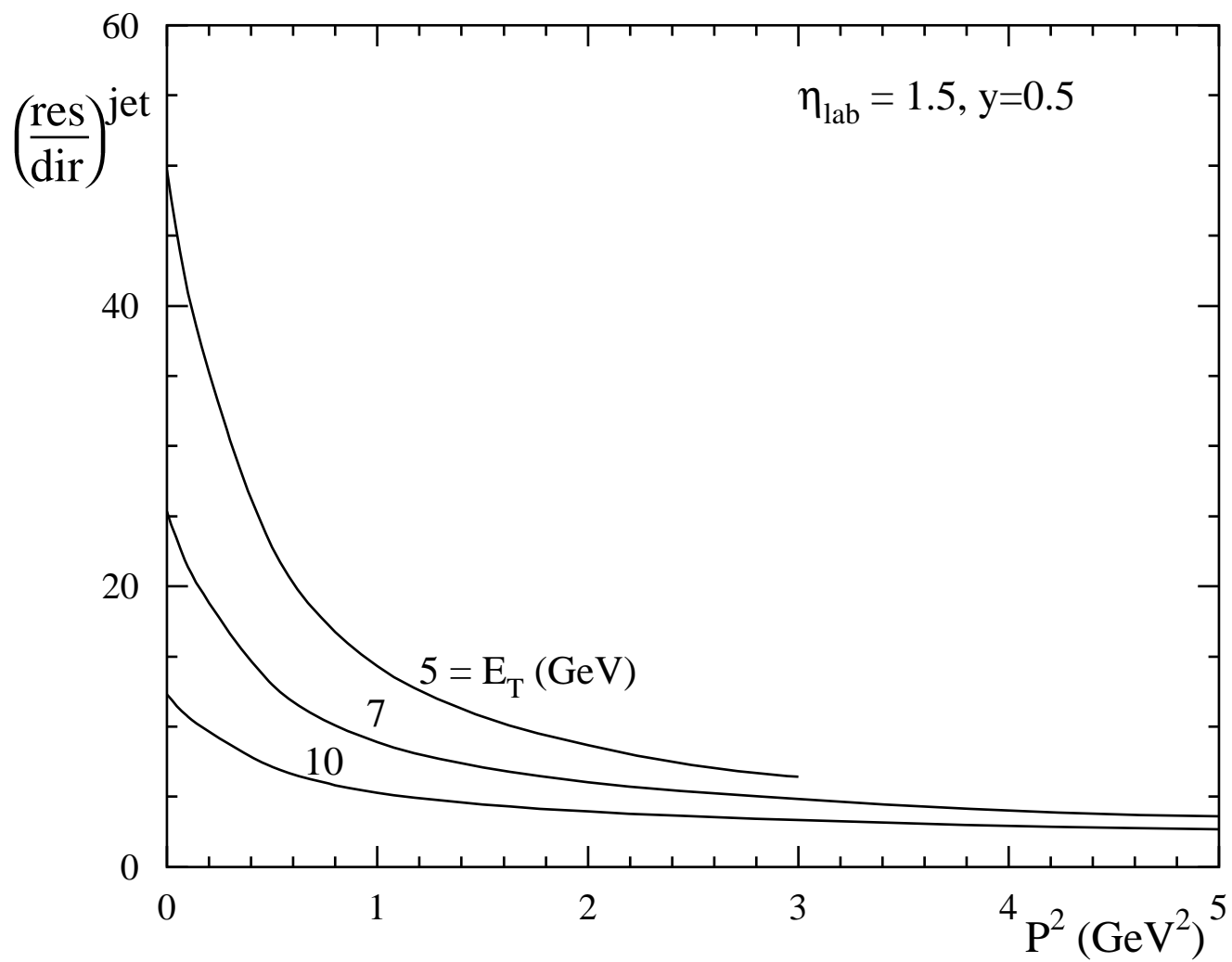


Fig. 5

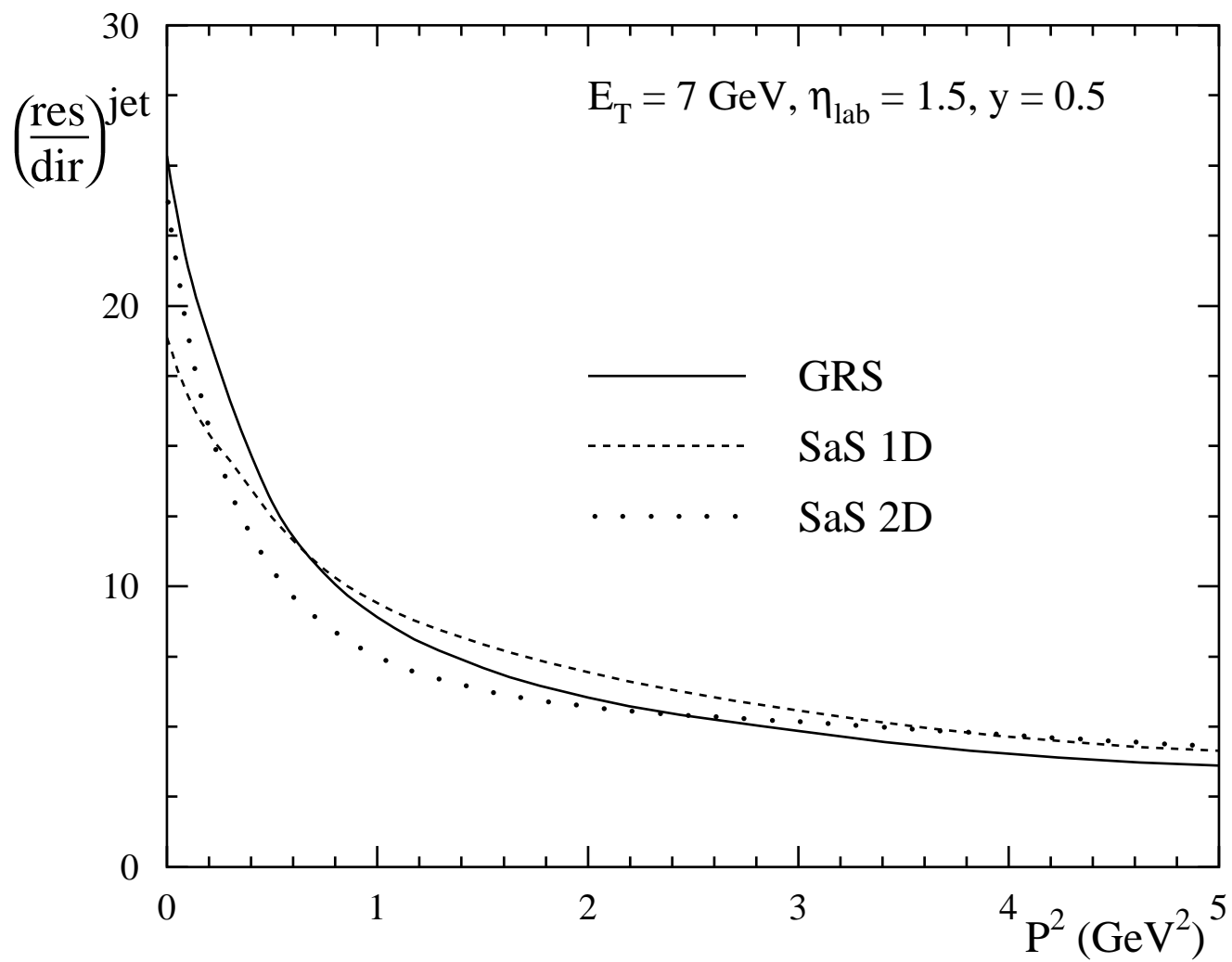


Fig. 6